Latin American Journal of Solids and Structures
www.lajss.org

Crashworthiness Analysis and Evaluation of Fuselage Section with Sub-floor Composite Sinusoidal Specimens

Abstract

Crashworthiness is one of the main concerns in civil aviation safety particularly with regard to the increasing ratio of carbon fiber reinforced plastic (CFRP) in aircraft primary structures. In order to generate dates for model validations, the mechanical properties of T700/3234 were obtained by material performance tests, and energy-absorbing results were gained by quasi-static crushing tests of composite sinusoidal specimens. The correctness of composite material model and single-layer finite element model of composite sinusoidal specimens were verified based on the simulation results and test results that were in good agreement. A typical civil aircraft fuselage section with composite sinusoidal specimens under cargo floor was suggested. The crashworthiness of finite element model of fuselage section was assessed by simulating the vertical drop test subjected to 7 m/s impact velocity, and the influences of different thickness of sub-floor composite sinusoidal specimens on crashworthiness of fuselage section were also analyzed. The simulation results show that the established finite element model can accurately simulate the crushing process of composite sinusoidal specimens; the failure process of fuselage section is more stable, and the safety of occupants can be effectively improved because of the smaller peak accelerations that was limited to human tolerance, a critical thickness of sub-floor composite sinusoidal specimens can restrict the magnitude of acceleration peaks, which has certain reference values for enhancing crashworthiness capabilities of fuselage section and improving the survivability of passengers.

Keywords

Crashworthiness; finite element method; composite sinusoidal specimens; energy-absorbing characteristic; fuselage section; failure modes; acceleration responses.

H.L. Mou *
T.C. Zou
Z.Y. Feng
J. Xie

Tianjin Key Laboratory of Civil Aircraft Airworthiness and Maintenance, Civil Aviation University of China, Tianjin, China

Author email：mhl589@163.com

http://dx.doi.org/10.1590/1679-78252446

Received 07.09.2015
In revised form 22.02.2016
Accepted 23.02.2016
Available online 27.02.2016

1 INTRODUCTION

Crashworthiness design, verification and airworthiness certification of transport category airplanes are significantly important for civil aviation safety, and the survivability of passengers and crews can be further improved through the crashworthiness design of aircraft, such as the structures of aircraft fuselage section, cabin layout and internal facilities (Abramowitz, 2002; Jackson, 2002; Jackson, 2008; Xue, 2014). However, there are new demands and huge challenges for the crashworthiness design, verification and airworthiness certification of composite aircraft structures with the extensive application of composite structures, due to the complex failure mechanisms, the energy-absorbing characteristic and crushing process of composite materials. The crashworthiness design and verification of composite aircraft structures mainly rely on the engineering experiences combined with extensive tests for a long period of time, but there are some disadvantages for the method, such as the long design cycles, high costs, poor repeatability etc. With the development of commercial finite element software codes, such as LS-DYNA, MSC.Dytran, ABAQUS and PAM-CRASH, an effective way to research the crashworthiness of composite aircraft structures is by using the numerical simulation methods combined with small amount of tests (Damodar, 2005; Feng, 2013; Heimbs, 2013; Wiggenraad, 1999; Xue, 2014; Zou, 2012). Therefore, in order to meet the requirements, the establishment and development of simulation analysis method on crashworthiness of fuselage section has become an important research work.

The crashworthiness design and certification of composite aircraft structures had been studied earlier by the United States and the Europe Union. The full-scale crash tests of composite aircrafts, such as Beech Starship, CirrusSR-20 and Lancair etc, were carried on by NASA (National Aeronautics and Space Administration) Langley Research Center in the early 1990s. Terry's (1997, 2000) results showed that these composite aircrafts had perfect crashworthiness capabilities. On September 8, 2009, FAA (Federal Aviation Administration) issued Advisory Circular AC 20-107B "composite aircraft structure" based on the researches, and presented airworthiness certification guidance information and acceptable compliance means about the crashworthiness of composite aircraft structures involving fiber reinforced materials. AIRBUS was participated in the CRASURV (The Design for Crash Surability) program that supported by the European Union. The Netherlands NLR (National Aerospace Laboratory) manufactured the composite sinusoidal specimen, and was responsible for the static tests, the German DLR (Deutsches Zentrum für Luft- und Raumfahrt) was responsible for the dynamic crushing tests, while the France CEAT (Centre d'Essais Aéronautiques de Toulous) carried out the crashworthiness tests of A320 fuselage section with subfloor composite sinusoidal specimens, and eventually put forward a complete set of crashworthy test methods for composite aircraft based on the crashworthiness researches (Wiggenraad, 2001). At the same time, the research institutes and scholars had done a lot of researches of composite aircraft structures with the combination methods of test and simulation with varying degrees of success, for circular tubes (Huang, 2009; Mamalis, 2006) square tubes (Palanivelu, 2010; Xiao, 2009), C channels (Deleo, 2009), and fuselage section (Jackson, 2011; Ilcewicz, 2005; Zou, 2012; Waimer, 2013; Feng, 2013). Based on the "building block" approach of FAA AC 20-107B, amount of experiments, simulation and optimization design studies of cargo subfloor composite C channels were conducted by JAMS (Joint Advanced Materials & Structures Center of Excellence) (Feraboli, 2008; Wade, 2011), the failure process and failure modes of composite C channels can be more accurately simulated by the developed finite element models, the tests and

simulation of details, sub-components and components would be further carried out in order to deeply study the crashworthy performance of composite fuselage section. The ONERA-Lille and AIRBUS France had redesigned the fuselage frames, and the energy-absorbing sinewave beams were located in the under-floor part of fuselage section, but failure modes were undesired based on the crashworthy tests and simulation of the redesigned fuselage section (David, 2004). So the crashworthiness of composite fuselage section need to be further studied with the increasing use of composite material structures in aircraft fuselage section.

The combination methods of test and simulation were used to research the energy-absorbing characteristic of composite sinusoidal specimens based on the mechanical properties of composite materials T700/3234 and quasi-static crushing results of composite sinusoidal specimens. At the same time, the single-layer finite element model of composite sinusoidal specimen was developed in HyperMesh, and the correctness of composite material model and finite element model of composite sinusoidal specimens were verified. The finite element model of fuselage section with sub-floor composite sinusoidal specimens was further built, and the composite sinusoidal specimens were arranged transversely in the fuselage frame plane. The failure modes and acceleration responses of fuselage section subjected to 7 m/s vertical impact velocity had been obtained and analyzed, and the influences of different thickness of composite sinusoidal specimens on crashworthiness of fuselage section were also researched.

2 CRUSHING TEST AND SIMULATION ANALYSIS OF COMPOSITE SINUSOIDAL SPECIMEN

2.1 Crushing Test of Composite Sinusoidal Specimen

The preparation and performance tests of composite sinusoidal specimen were conducted in AVIC Beijing Institute of Aeronautical Materials. The composite sinusoidal specimen is 76.2 mm long, 50.80 mm wide from end-lip to end-lip, and 2 mm thick. The detailed dimensions is shown in Figure1 (a), and the composite sinusoidal specimen is shown in Figure1 (b). The 45-degree chamfer sided weakness is set up at the top of the composite sinusoidal specimen in order to initiate steady crush. The material system is T700 carbon fiber/3234 epoxy prepreg, it is a unidirectional tape 12k tow, and a 270 ℉ (132 ℃) cure resin designated for autoclave or oven-only cure. The composite sinusoidal specimen consists of 16 layers of unidirectional laminates with orientations $[0^\circ/90^\circ]_{4s}$, and each layer thickness is 0.125 mm. The uniform crushing rate is 2.5 mm/min, and the typical morphology of composite sinusoidal specimen after crush testing and the quasi-static crushing load-displacement curve are shown in Figure2 and Figure3, respectively.

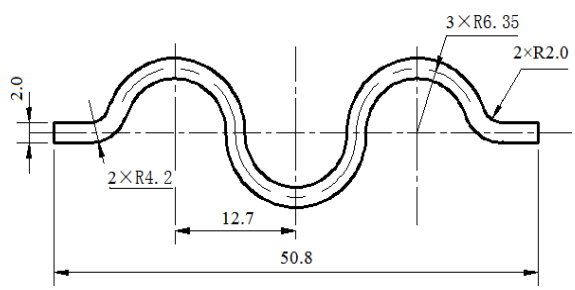

(a) Sectional geometry

(b) Composite sinusoidal specimen

Figure 1: Composite sinusoidal specimen.

Figure 2: Typical morphology of composite sinusoidal specimen after crush testing.

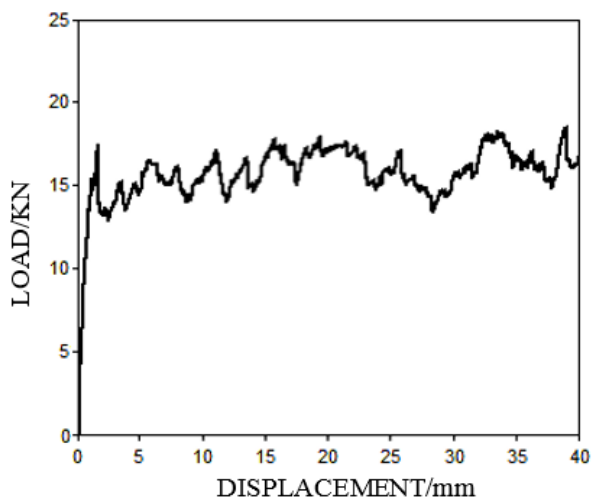

Figure 3: Quasi-static crushing load-displacement curve.

Specific Energy Absorption (*SEA*): The energy absorbed per unit mass of crushed structure. The ability of material to dissipate energy can be expressed in terms of *SEA*, which has units of J/g. Setting the mass of structure that undergoes crushing as the product of stroke *l*, cross-sectional area A, and density ϱ:

$$SEA = \frac{E_A}{m} = \frac{\int Fdl}{m} = \frac{\int Fdl}{\rho \cdot A \cdot l} \tag{1}$$

The calculating *SEA* value is 72.47 J/g for the composite sinusoidal specimen.

2.2 Finite Element Model

The LS-DYNA model is represented in Figure 4, and shows the rigid ground, the composite sinusoidal specimen and the trigger row. The shell element is commonly used in crashworthiness simulation of aircraft fuselage section, and the fully integrated shell element (formulation 16) is adopted for the finite element model of composite sinusoidal specimen because it can simulate bucking accurately, calculate internal energy absorption accurately, and calculate vary fast (Paolo, 2011; LSTC, 2012). The finite element model of composite sinusoidal specimen is modeled with total of 840 shell elements of 2.54 mm×2.54 mm, having constant thickness of 2 mm. The 45-degree chamfer is modeled as a single row of reduced thickness 0.25 mm elements at the crush front of the specimen.

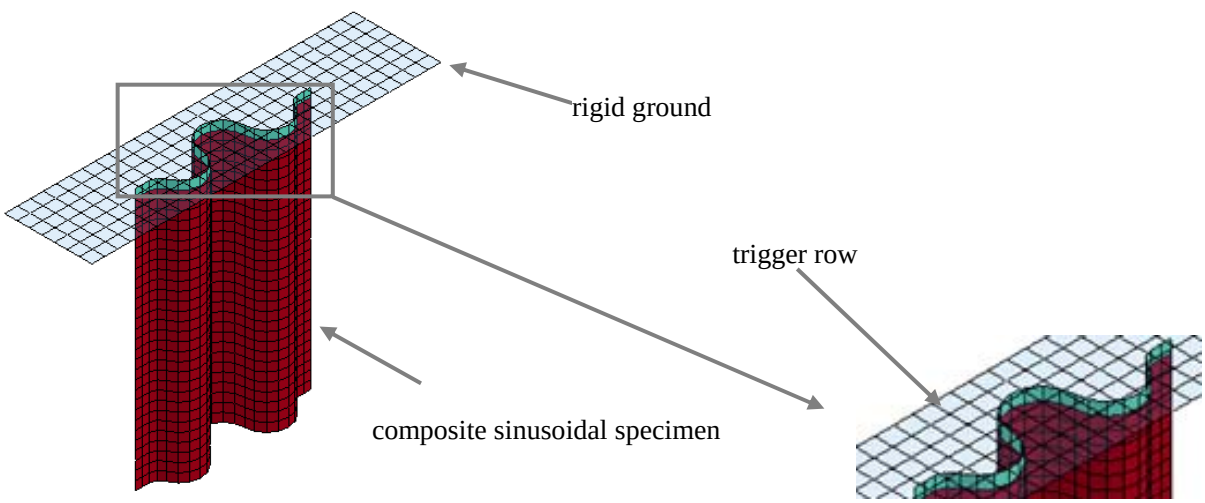

Figure 4: Finite element model of rigid ground, composite sinusoidal specimen, and trigger row .

The card * PART_COMPOSITE is used to define the 16 layers of composite sinusoidal specimen, and the finite element model is adopted the material model of MAT 54_Enhanced_Composite_Damage, which used the Chang-Chang failure criterion in the LS-DYNA theoretical manual (Han, 2007; LSTC, 2012). The material card of MAT 54 contains input parameters for both material physical properties of T700/3234 (Table 1) and other code-specific parameters (Table 2) (Paolo, 2011; LSTC, 2012). The material physical properties of T700/3234

are obtained from the material tests according to the CMH-17G (CMH-17 Working Group, 2012). The material model of MAT 20_Rigid is selected for rigid ground, and the input parameters of material card of MAT 20 are shown in Table 3 (LSTC, 2012).

Symbol	Title	Value
ϱ	Density	1.53 g/cm^3
E_a	Young's modulus in longitudinal (fiber) direction	128 GPa
E_b	Young's modulus in transverse (perpendicular to fiber) direction	8.4 GPa
G_{ab}	Shear modulus in *ab* plane	4.0 GPa
G_{bc}	Shear modulus in *bc* plane	4.0 GPa
G_{ca}	Shear modulus in *ac* plane	4.0 GPa
P_{rab}	Minor Poisson's ratio	0.0218
X_t	Longitudinal tensile strength (fiber direction)	2093 MPa
X_c	Longitudinal compressive strength (fiber direction)	1060 MPa
Y_t	Transverse tensile strength (perpendicular to fiber)	50 MPa
Y_c	Transverse compressive strength (perpendicular to fiber)	198 MPa
S_c	Shear strength in *ab* plane	104 MPa

Table 1: Material physical properties of T700/3234.

Symbol	Title	Value
DFAILT	Max strain for fiber tension	0.0174
DFAILC	Max strain for fiber compression	-0.02
DFAILM	Max strain for matrix straining in tension and compression	0.024
DFAILS	Max shear strain	0.03
BETA	Weighing factor for shear term in tensile fiber mode	0.5
FBRT	Softening factor for fiber tensile strength after matrix failure	0.5
YCFAC	Softening factor for fiber compressive strength after matrix failure	1.2
TFAIL	Time step size criteria for element deletion	1.153e-9
SOFT	Crush front strength reducing parameter	0.70
EFS	Effective failure strain	0

Table 2: The other code-specific parameters of MAT 54.

Symbol	Title	Value
ϱ	Density	7.9 g/cm^3
E	Modulus of elasticity	210 GPa
μ	Poisson's ratio	0.3

Table 3: The input parameters of material card of MAT 20.

2.3 Material Damage Model

For the MAT54_Enhanced_Composite_Damage material model in LS-DYNA, the material stress-strain curves in the elastic region is as follows:

$$\varepsilon_{aa} = \frac{1}{E_a}(\sigma_{aa} - \nu_{ab}\ \sigma_{bb}) \tag{2}$$

$$\varepsilon_{bb} = \frac{1}{E_b}(\sigma_{bb} - \nu_{ba}\ \sigma_{aa}) \tag{3}$$

$$2\varepsilon_{ab} = \frac{1}{G_{ab}}\ \tau_{ab} + \alpha\ \tau^{3}_{ab} \tag{4}$$

The Chang-Chang failure criterion is used to determine the behavior of MAT54 material (Chang, 1987; Han, 2007; Paolo, 2011; LSTC, 2012), if the material is beyond the elastic region, as follows:

(a) for the tensile fiber mode:

$$\sigma_{aa} > 0,\quad e_f^2 = \left(\frac{\sigma_{aa}}{X_t}\right)^2 + \beta\left(\frac{\sigma_{ab}}{S_c}\right) - 1 \begin{cases} \geq 0, \textit{ failed} \\ < 0, \textit{elastic} \end{cases} \tag{5}$$
$$E_a = E_b = G_{ab} = \nu_{ba} = \nu_{ab} = 0$$

(b) for the compressive fiber mode:

$$\sigma_{aa} < 0,\quad e_c^2 = \left(\frac{\sigma_{aa}}{X_c}\right)^2 - 1 \begin{cases} \geq 0, \textit{ failed} \\ < 0, \textit{elastic} \end{cases} \tag{6}$$
$$E_a = \nu_{ba} = \nu_{ab} = 0$$

(c) for the tensile matrix mode:

$$\sigma_{bb} > 0,\quad e_m^2 = \left(\frac{\sigma_{bb}}{Y_t}\right)^2 + \left(\frac{\sigma_{ab}}{S_c}\right) - 1 \begin{cases} \geq 0, \textit{ failed} \\ < 0, \textit{elastic} \end{cases} \tag{7}$$
$$E_a = \nu_{ba} = 0 \rightarrow G_{ab} = 0$$

(d) for the tensile fiber mode:

$$\sigma_{bb} < 0,\quad e_d^2 = \left(\frac{\sigma_{bb}}{2S_c}\right)^2 + \left[\left(\frac{Y_c}{2S_c}\right)^2 - 1\right]\frac{\sigma_{bb}}{Y_c} + \left(\frac{\sigma_{ab}}{S_c}\right) - 1 \begin{cases} \geq 0, \textit{ failed} \\ < 0, \textit{elastic} \end{cases} \tag{8}$$
$$E_a = \nu_{ba} = \nu_{ab} = 0 \rightarrow G_{ab} = 0$$

2.4 Simulation and Validation of Finite Element Model

For the finite element model of composite sinusoidal specimen, the specimen is kept at rest by constraining all freedom degrees of the bottom row of nodes opposite the crush trigger, and the top nodes of the crush trigger are completely free. The different loading speeds of rigid ground are 38 mm/s, 380 mm/s and 3800 mm/s, respectively. The simulation load-displacement curves are shown in Figure 5.

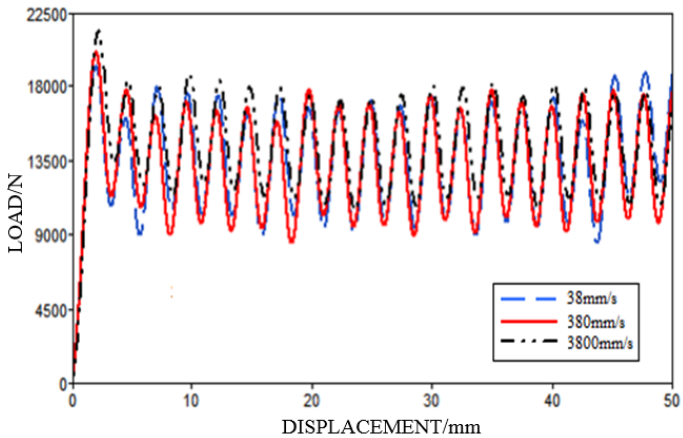

Figure 5: Load-displacement curves under different velocities.

As can be seen from Figure 5, there are little effects on peak loads, average crush loads, overall load-displacement responses and the absorbed energy regardless of the strain rate effects for different loading speeds. Solution time takes 4 minutes using a workstation with a 2.26 GHz dual Quad-core (8 processors) 64-bit 16 GB RAM computer when the loading speed of rigid ground is 3800 mm/s. The different solution times are listed in Table 4, the computational efficiency is significantly improved with the increasing of the loading speeds. Through a sensitivity study, the loading speed of 3800 mm/s is reasonable.

Loading speed/mm • s^{-1}	Solution time/min
3800	4
380	44
38	428

Table 4: Solution time under different loading speeds.

The Rigid_Nodes_to_Rigid_Body Contact algorithm is selected to define the contact relationships between the rigid ground and composite sinusoidal specimen. The simulation failure modes of composite sinusoidal specimen, as shown in Figure 6, reveal that failure advances in an even and stable mode, through elements deletion at the crush front. When the first ply in an element fails, the elements remain in the straight position and do not exhibit a different morphology. Once all

plies fail, the elements are immediately deleted. Once an element is deleted, the entire row of elements is also deleted. Therefore, the crush progresses with a progressive deletion of the crush front row of elements are achieved without any other graphic indication.

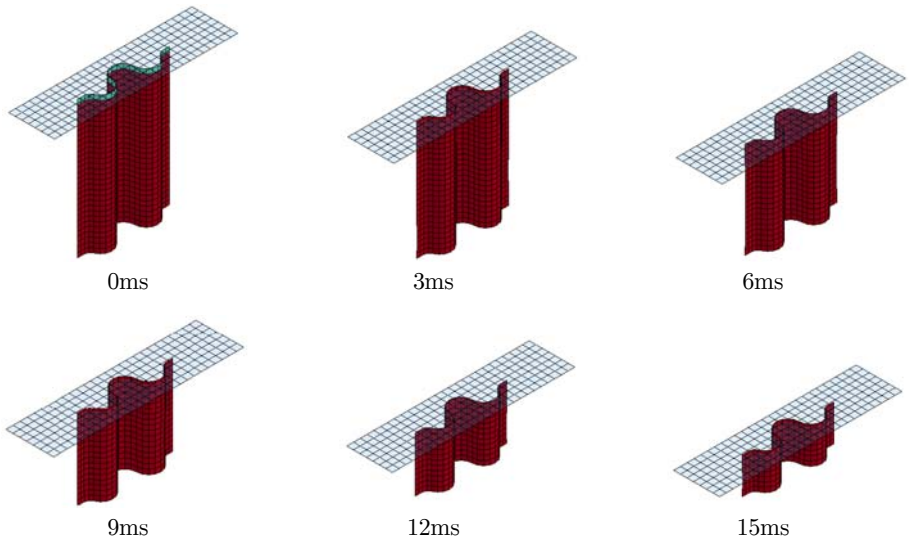

Figure 6: Time progression of the baseline simulation showing stable element row deletion.

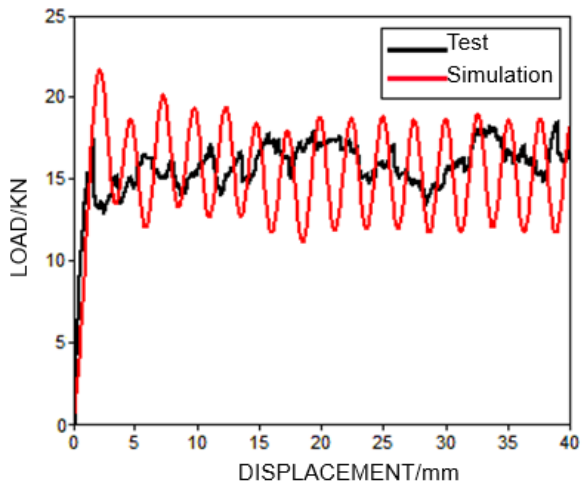

Figure 7: Experimental and model baseline load-displacement curves.

A low-pass digital filter (SAE 600 Hz) is used to filter numeric results during the post-processing (Xiao, 2009; Feraboli, 2010), and the filtered simulation load-displacement curve is compared with the experimental curve in Figure 7. The simulation captures the key characteristics of experimental curve: peak load, average crush load, and *SEA* value. The predicted *SEA* value is 69.98 J/g, compared to the experimental 72.47 J/g, the difference is -3.44% which is within a little and acceptable range. The material model MAT 54 of composite sinusoidal specimen can captures all the experimental significant

features, and the simulation *SEA* value is highly agreed with the experimental value, which can validate the correctness of finite element model, so the material model MAT 54 can also be used to successfully simulate the behavior of composite sinusoidal specimens undergoing axial crushing. Therefore, the composite sinusoidal specimens are used as sub-floor energy-absorbing structures of fuselage section, and the crashworthiness simulation analysis of fuselage section are further conducted based on the finite element model of composite sinusoidal specimen.

3 FINITE ELEMENT MODEL OF FUSELAGE SECTION

The finite element model of fuselage section with sub-floor composite sinusoidal specimens was built by using the computer software code HyperMesh (Han, 2007; Zou, 2012; Altair Engineering, 2013; Feng, 2013; Siromani, 2013), due to the aircrafts deformation mainly occured in fuselage sub-floor structure during a crash. The finite element model of fuselage section consisted of skin, fuselage frames, long stringers, oblique struts, floor beams, floor composite sinusoidal specimen, and so on. The length of finite element model of fuselage section was 1200 mm, and the radius of cargo compartment was 1600 mm. The fuselage frames were redesigned, and the chosen design for fuselage section was represente on Figure 8, the composite sinusoidal specimens were horizontal arrangement among the frames and skin.

Because of large size and complexity of real fuselage section structures, the finite element model was reasonably simplified during the modeling process of fuselage section based on the simplified principles described by Adam (2003) and Ikuo (2000), the rivets, screws, windows, doors and cargo were ignored. The masses of seats and dummies were accounted as concentrated masses located at the junctions between seats and floor, as shown in Figure 8, the concentrated mass of each seat and dummy was defined to 88 kg according to Federal Aviation Regulation 25.562(b). The material model of rigid ground was selected to MAT 20_Rigid. The overall finite element model of fuselage section consisted of 184944 nodes and 180965 elements. The Belytschko-Tsay shell element had been adopted because the shell element could accurately and effectively simulate buckling and calculate internal energy absorption.

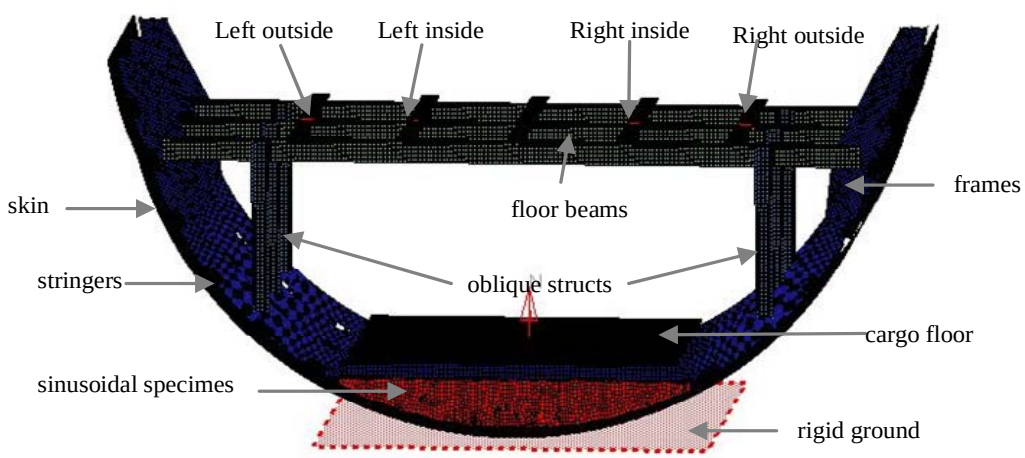

Figure 8: Finite element model of fuselage section.

In addition to composite sinusoidal specimens, the rest structures of fuselage section were made of aluminum alloy. Al 2024 was used for cargo floor and skin. Al 7075 was used for frames, stringers, seat tracks, floor beams and oblique struts. Aluminum alloy adopted the MAT 24 material model with the bilinear elastic–plastic properties, and the mechanical properties was shown in Table 5 (LSTC, 2012; Zou, 2012). The explicit dynamics finite element algorithm was used for the MAT 24 material model. The Belytschko-Tsay shell element would be failed if the effective strain reached the maximum plastic strain, and the yielding model of shells were the Von-Mises stress model. The vertical crash direction of finite element model was parallel to the normal direction of rigid wall, and the vertical impact velocity of 7 m/s was selected to evaluate the crashworthiness of fuselage section without considering aerodynamic force. Based on the penalty algorithm, Automatic_Single_Surface_Contact was used to define the contact relationships among skin, fuselage frames and rigid ground.

Material	Density/ $kg{\cdot}m^{-3}$	Modulus of elasticity/ GPa	Poisson's ratio	Yield modulus/ MPa	Enhanced modulus/ MPa	Maximum strain failure criteria
Al 2024	2796	71	0.33	469	852	0.08
Al 7075	2768	71	0.35	269	908	0.15

Table 5: The aluminum mechanical properties.

4 CRASHWORTHINESS SIMULATION ANALYSIS OF FUSELAGE SECTION

4.1 Failure Modes

Figure 9 and Figure 10 show the stress cloud and deformation contour of fuselage section with composite sinusoidal specimens under cargo floor at different times. As can be seen from Figure 9(a) and Figure 10(a), the fuselage bottom section firstly crashes with the rigid ground, the composite sinusoidal specimens exhibit stable and progressive element failure and deletion because of the larger upward in-plane loads. The skin is subjected to outward tensile loads and the destruction process of fuselage section is more stable. As can be seen from Figure 9(b) and Figure 10(b), the composite sinusoidal specimens substantially completely destroy, and the fuselage frames begin to crash with rigid ground and the skin wrinkles slightly. As can be seen from Figure 9(c) and Figure 10(c), the skin wrinkles seriously, the cargo floor raises upward to the direction of cabin floor, and withstands the tensile loads. The oblique struts crash with rigid ground, resulting in inward bending rupture of fuselage frames. The larger deformations occur in the junctions between the oblique struts and fuselage frames, which lead to two plastic hinges which has been marked in the Figure 9(c), and the cabin floor is not penetrated by oblique struts.

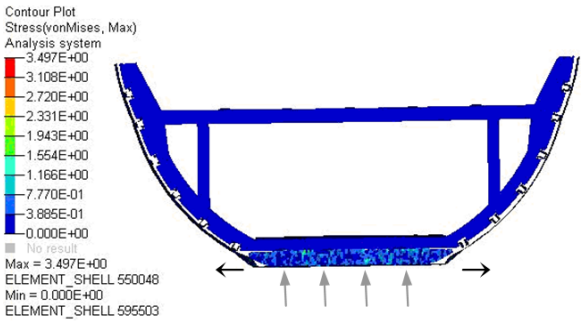

(a) 20ms

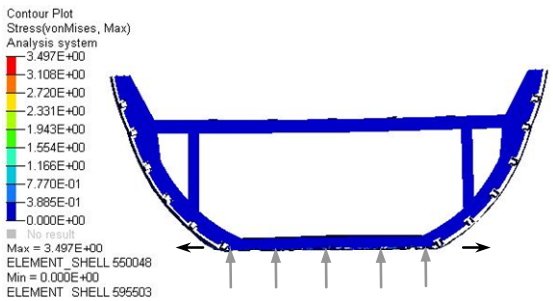

(b) 40ms

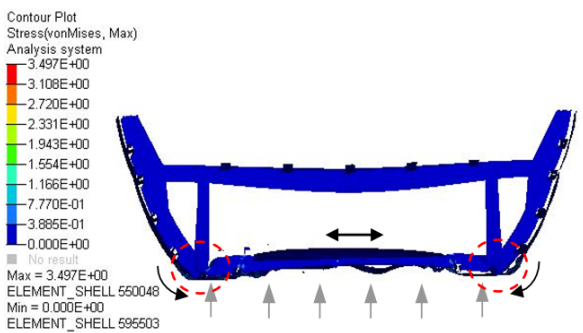

(c) 120ms

Figure 9: The stress cloud of composite fuselage section at different times.

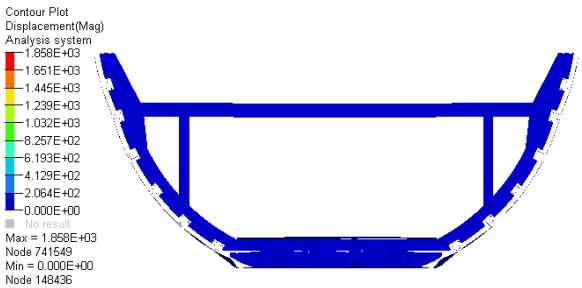

(a) 20ms

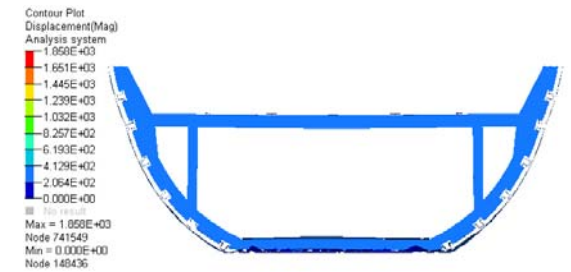

(b) 40ms

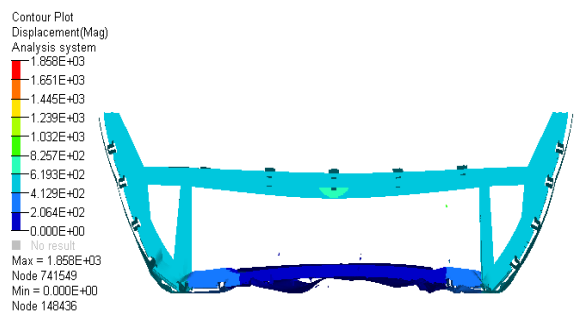

(c) 120ms

Figure 10: The deformation contour of composite fuselage section at different times.

4.2 Acceleration Response Characteristics

The acceleration characteristic is one of the important factors for occupants' safety and can be evaluated with the acceleration at junctions between seats and floor. The sampling frequency is set as SAE 600 Hz. Figure 11 shows the acceleration history curves of junctions between seats and floor. As can be seen from Figure 11, the trends of acceleration response between insides and outsides seats are more consistent, and the acceleration peaks of outside seats are slightly larger than that of inside seats. This is because of the rigid triangular area within fuselage frames, cabin floor and its supporting beams, which led to the slightly larger acceleration peaks at the outside seats and floor connections.

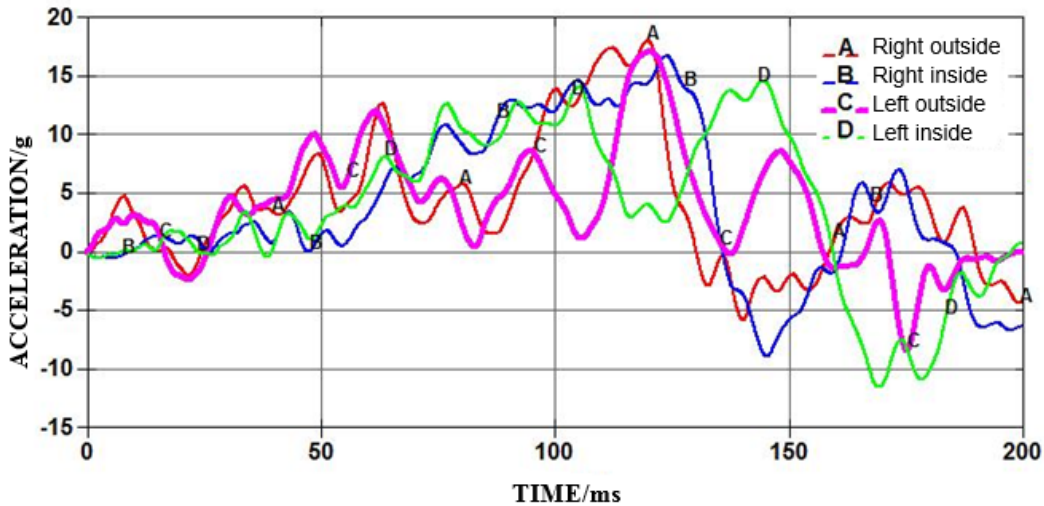

Figure 11: Acceleration responses of the junctions between seats and floor.

	Left outside	Left inside	Right inside	Right outside
Positive peak acceleration corresponding time	17 g 120 ms	15 g 145 ms	16.5 g 130 ms	18 g 120 ms
Negative peak acceleration corresponding time	-8 g 175 ms	-11.5 g 170 ms	-8.5 g 145 ms	-5.5 g 140 ms

Table 6: Maximum peak acceleration and corresponding time.

The maximum peak acceleration and corresponding times for the four different seat reference points are shown in Table 6. The acceleration is smaller before 40 ms because the impact kinetic energy is well dissipated by the progressive failure of composite sinusoidal specimens and damaged skin. The acceleration is gradually increased after 40 ms because the metal fuselage frames are in contact with rigid ground. The acceleration is maximized at around 120 ms because the oblique struts of cabin floor are in contact with rigid ground. The corresponding 18 g maximum positive peak acceleration appears in 120 ms for the right outside reference point, while the corresponding -11.5 g maximum negative peak acceleration appears in 170 ms for the left inside reference point. The human tolerance limits to acceleration are shown in Table 7 from JSSG-2010-7 crew systems crash protection hand-book (1998). As can be seen, the maximum positive peak acceleration (eyeballs down) does not exceed the tolerance level of 25 g, and the maximum negative peak acceleration (eyeballs up) does not exceed the tolerance level of -15 g. The acceleration are limited to human tolerance, which can ensure the safety of occupants.

Direction of accelerative force	Occupant's inertial response	Tolerance level
Headward	Eyeballs down	25 g
Tailward	Eyeballs up	-15 g

Table 7: Human tolerance limits to acceleration (JSSG-2010-7, 1998).

5 INFLUENCE OF DIFFERENT THICKNESS OF COMPOSITE SINUSOIDAL SPECIMENS ON CRASHWORTHINESS OF FUSELAGE SECTION

It is clear that the stiffness and stress of sub-floor composite sinusoidal specimens has a great effect on acceleration response characteristics of the fuselage section, though the sub-floor composite sinusoidal specimens are not the main energy-absorbing component. The simulated acceleration variation of fuselage section with different thickness of sub-floor composite sinusoidal specimens is plotted in Figure 12, and the thickness of sub-floor composite sinusoidal specimens is varied as 1 mm, 1.5 mm, 2.0 mm, 2.5 mm, and 3 mm, respectively.

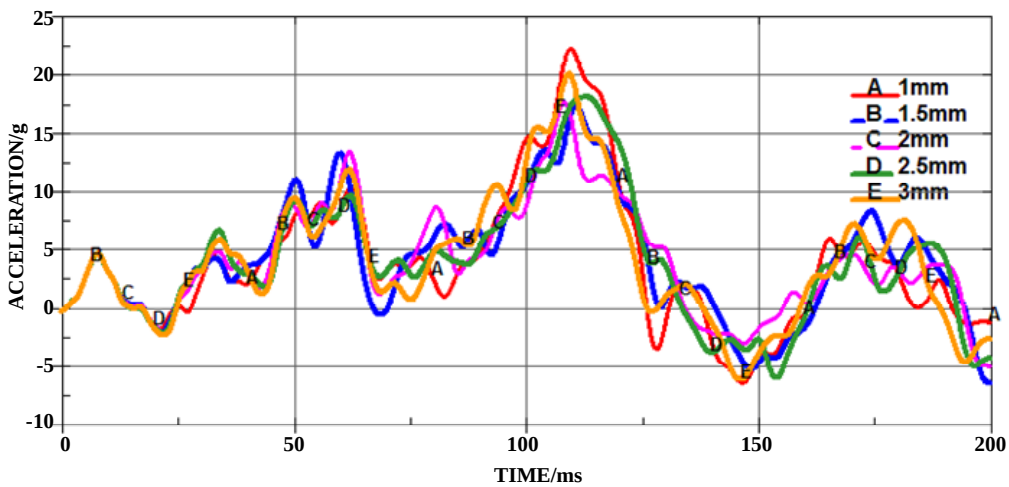

Figure 12: Acceleration responses of different thickness of sub-floor composite sinusoidal specimens.

The maximum peak acceleration of fuselage section with different thickness of sub-floor composite sinusoidal specimens are obtained from Figure 12, and the maximum peak acceleration of fuselage section are shown in Figure 13. It is obvious that when the sub-floor composite sinusoidal specimens are weaker (e.g. the thickness is 1.0 mm), the peak acceleration is relatively higher, i.e. 22.5 g. When the sub-floor composite sinusoidal specimens are more rigid and stronger (e.g. the thickness are 1.5 mm and 2 mm), the peak acceleration is relatively lower, as shown in Figure 13. However, if the sub-floor composite sinusoidal specimens are too rigid (e.g. the thickness is 3.0 mm), the peak acceleration is relatively higher, i.e. 20.4 g. When the thickness of sub-floor composite sinusoidal specimens is 1.5 mm in the five selected thickness, the maximum peak acceleration is the lowest, i.e.

17.6 g. Therefore, the thickness of sub-floor composite sinusoidal specimens can limit the magnitude of peak acceleration.

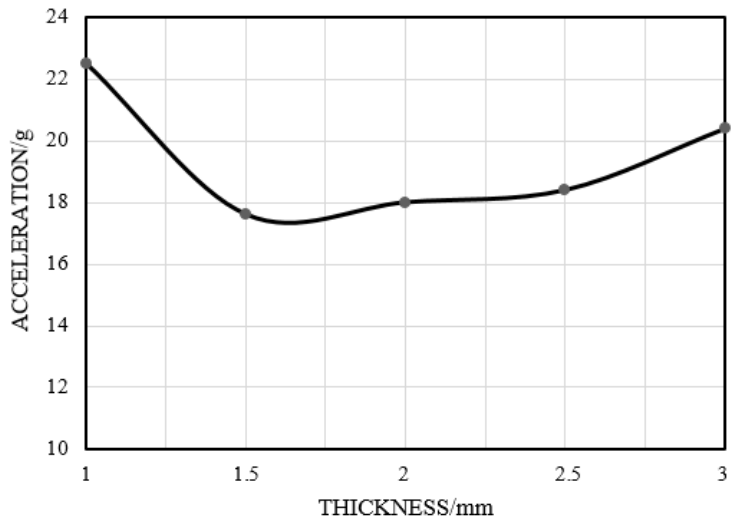

Figure 13: Maximum peak acceleration with different thickness of sub-floor composite sinusoidal specimens.

6 CONCLUSIONS

The failure behaviors of composite sinusoidal specimens are researched based on the combination of methods of test and simulation, and the crashworthiness of fuselage section with composite sinusoidal specimens under cargo floor are further studied based on the composite material model and finite element model. The main conclusions are listed as follows:

(1) The mechanical properties parameters of T700/3234 are obtained by the performance tests, the energy-absorbing results of composite sinusoidal specimens are achieved by the crushing tests. The single-layer finite element model of composite sinusoidal specimen can accurately simulate the initial peak load, load-displacement curve and the SEA value, but the single-layer approach can provide no insight into the failure process.

(2) The composite sinusoidal specimens are used as sub-floor energy-absorbing structures of fuselage section. The failure process of fuselage section is more stable because of the progressive failure of composite sinusoidal specimen, and the cabin floor is not penetrated by oblique struts.

(3) The acceleration is smaller in the earlier crash process because of the progressive failure of composite sinusoidal specimens. The acceleration is gradually increased in the later crash process because the oblique struts are in contact with rigid ground. However, the maximum positive peak acceleration does not exceed 25 g, and the maximum negative peak acceleration does not exceed -15 g, which can ensure the safety of occupants.

(4) The local stiffness and strength of sub-floor composite sinusoidal specimens have significant influence on peak acceleration of fuselage section. With the increase of thickness of sub-floor composite sinusoidal specimens, the peak acceleration first decreases, and then

increases. A critical thickness of sub-floor composite sinusoidal specimens can restrict the magnitude of peak acceleration of fuselage section, which can greatly improve the survivability of passengers.

Acknowledgement

The authors acknowledge the supports from Science and Technology Item from Civil Aviation Administration of China (MHRD20140207), Fundamental Research Funds for the Central Universities (3122015D022), and Fund of Tianjin Key Laboratory of Civil Aircraft Airworthiness and Maintenance in Civil Aviation University of China.

References

Abramowitz, A., Smith, T. G., Vu, T., Zvanya, J., (2002). Vertical drop test of a narrow-body transport fuselage section with overhead stowage bins, Report Number DOT/FAA/AR-01/100.

Adams, A., Lankarani, H. M., (2003). A modern aerospace modeling approach for evaluation of aircraft fuselage crashworthiness. International Journal of Crashworthiness 8(4): 401-413.

Altair Engineering, (2014). Hypermesh user's guide. Altair Engineering Inc.

Chang, F. K., Chang, K. Y., (1987). A progressive damage model for laminated composites containing stress concentration. Journal of Composite materials (21): 834-855.

CMH-17 Working Group, (2012). Composite Materials Handbook (CMH-17G), Volume 1 Guidelines for characterization of structural material, Release G.

Damodar, R. A., Marshall, R., (2005). Design and evaluation of composite fuselage panels subjected to combined loading conditions. Journal of Aircraft 42(4):1037-1045.

David, D., Didier, J., Michel, M., Gérard, W., (2004) Evaluation of finite element modeling methodologies for the design of crashworthy composite commercial aircraft fuselage. 24th International Congress of the Aeronautical Sciences. Department of defense joint service specification guide. (1998). JSSG-2010-7 crew systems crash protection handbook.

Deleo, F., Wade, B., Feraboli, P., Rassaian, M., (2009). Crashworthiness of Composite Structures: Experiment and Simulation. Proceedings of the 50th AIAA Structures, Structural Dynamics and Materials Conference, Palm Springs, CA, May 4-7.

Feng, Z. Y., Mou, H. L., Zou, T. C., Ren, J., (2013). Research on effects of composite skin on crashworthiness of composite fuselage section. International Journal of Crashworthiness 18(5): 459-464.

Feraboli, P., (2008). Development of a corrugated test specimen for composite materials energy absorption. Journal of Composite Materials 42(3): 229-256.

Feraboli, P., Rassaian, M., (2010). Proceedings of the CMH-17 (MIL-HDBK-17) Crashworthiness Working Group Numerical Round Robin. Costa Mesa, CA.

Feraboli, P., Wade, B., Deleo, F., Rassaian, M., Higgins, M., Byar, A., (2011). LS-DYNA mat54 modeling of the axial crushing of a composite tape sinusoidal specimen. Composites: Part A 42: 1809-1825.

Han, H. P., Taheri, F., Pegg, N., Lu, Y., (2007). A numerical study on the axial crushing response of hybrid pultruded and $\pm 45^{\circ}$ braided tubes. Composite Structures (80): 253-264.

Heimbs, S., Hoffmann, M., Waimer, M., Schmeer, S., Blaurock, J., (2013). Dynamic testing and modelling of composite fuselage frames and fasteners for aircraft crash simulations. International Journal of Crashworthiness 18(4): 406-422.

Huang, J. C., Wang, X. W., (2009). Numerical and experimental investigations on the axial crushing response of composite tubes. Journal of Composite Structures 91: 222-228.

Ikuo, K., Masakatsu, M., Kazuo, I., (2000). Impact simulation of simplified structural models of aircraft fuselage. San Diego: 2000 World Aviation Conference 1-6.

Ilcewicz, L. B., Brian, M., (2005). Safety & certification initiatives for composite airframe structure. 46th AIAA/ASME/ ASCE/AHS/ASC structures, Structural Dynamics & Materials Conference, Austin, Texas.

Jackson, K. E., Fasanella, E. L., (2001). Development of a scale model composite fuselage concept for improved crashworthiness. Journal of Aircraft 38(1): 95-103.

Jackson, K. E., Fasanella, E. L., (2002). Crash simulation of vertical drop tests of two Boeing 737 fuselage sections, Report Number DOT/FAA/AR-02/62.

Jackson, K. E., Fasanella, E. L., (2008). Development and validation of a finite element simulation of a vertical drop test of an ATR 42 regional transport airplane, Report Number DOT/FAA/AR-08/19.

LSTC., (2012). LS-DYNA theoretical manual. California: Livermore Software Technology Corporation.

Mamalis, A. G., Manolakos, D. E., Ioannidis, M. B., Papapostolou, D. P., (2006). The static and dynamic axial collapse of CFRP square composite tubes: Finite element modeling. Journal of Composite Structures 74: 213-225.

Palanivelu, S., Paepegem, W., Degrieck, J., Kakogiannis, D., Ackeren, J., Hemelrijck, D., (2010). Parametric study of crushing parameters and failure patterns of pultruded composite tubes using cohesive elements and seam, Part I: Central delamination and triggering modeling. Polymer Testing 29: 729-741.

Paolo, F., Bonnie, W., Francesco, D., Mostafa, R., Mark, H., Alan, B., (2011). LS-DYNA MAT54 modeling of the axial crushing of a composite tape sinusoidal specimen. Composite: Part A 42: 1809-1825.

Siromani, D., (2013) Crashworthiness design and analysis of aircraft structures. Drexel University, Doctor of Philosophy 1-245. Terry, J. E., Hooper, S. J., Nicholson, M., (1997). Design and test of an improved crashworthiness small composite airframe–phase II report, NASA SBIR Contract NAS1-20427, Terry Engineering, Andover, Kansas.

Terry, J. E., (2000) Design and test of an improved crashworthiness small composite airplane, SAE Paper 2000-01-1673, Presented at the SAE General Aviation Technology Conference and Exposition, Wichita, KS.

Waimer, M., Kohlgruber, D., Hachenberg, D., Voggenreiter, H., (2013). Experimental study of CFRP components subjected to dynamic crash loads. Composite Structures 105: 288-299.

Wiggenraad, J. F. M., Michielsen, A. L. P. J., Santoro, D., Lepage, F., Kindervater, C., Beltran, F., (1999). Development of a crashworthy composite fuselage structure for a commuter aircraft, NLR-TP-99532.

Wiggenraad, J. F. M., Santoro, D., Lepage, F., Kindervater, C., Mañez, H. C., (2001). Development of a crashworthy composite fuselage concept for a commuter aircraft, NLR-TP-2001-108.

Xiao, X., (2009). Modeling energy absorption with a damage mechanics based composite material model. Journal of Composite Materials 43(5): 427-444.

Xiao, X., Botkin, M., Johnson, N. L., (2009). Axial crush simulations of braided carbon tubes using MAT58 in LS-DYNA. Thin-Walled Structures 38: 2247-2259.

Xue, P., Ding, M. L., Qiao, C. F., Xu, T. X., (2014). Crashworthiness study of a civil aircraft fuselage section. Latin American Journal of Solids and Structures 11(9):1615-1627.

Zou, T. C., Mou, H. L., Feng, Z. Y., (2012). Research on effects of oblique struts on crashworthiness of composite fuselage sections. Journal of Aircraft 49(6): 2059-2063.